Hindawi Publishing Corporation
International Journal of Photoenergy
Volume 2012, Article ID 928760, 9 pages
doi:10.1155/2012/928760

Research Article

Synthesis and Characterization of CeO_2-SiO_2 Nanoparticles by Microwave-Assisted Irradiation Method for Photocatalytic Oxidation of Methylene Blue Dye

R. M. Mohamed[1,2] and E. S. Aazam[1]

[1] *Chemistry Department, Faculty of Science, King Abdulaziz University, P.O. Box 80203, Jeddah 21589, Saudi Arabia*
[2] *Advanced Materials Department, Central Metallurgical Resarch and Devolpment Institute CMRDI, P.O. Box 8742, Helwan 11421, Egypt*

Correspondence should be addressed to R. M. Mohamed, redama123@yahoo.com

Received 12 March 2012; Revised 30 April 2012; Accepted 1 May 2012

Academic Editor: Pengyi Zhang

CeO_2-SiO_2 nanoparticles were synthesized for the first time by a facile microwave-assisted irradiation process. The effect of irradiation time of microwave was studied. The materials were characterized by N_2 adsorption, XRD, UV-vis/DR, and TEM. All solids showed mesoporous textures with high surface areas, relatively small pore size diameters, and large pore volume. The X-ray diffraction results indicated that the as-synthesized nanoparticles exhibited cubic CeO_2 without impurities and amorphous silica. The transmission electron microscopy (TEM) images revealed that the particle size of CeO_2-SiO_2 nanoparticles, which were prepared by microwave method for 30 min irradiation times, was around 8 nm. The photocatalytic activities were evaluated by the decomposition of methylene blue dye under UV light irradiations. The results showed that the irradiation under the microwave produced CeO_2-SiO_2 nanoparticles, which have the best crystallinity under a shorter irradiation time. This indicates that the introduction of the microwave really can save energy and time with faster kinetics of crystallization. The sample prepared by 30 min microwave irradiation time exhibited the highest photocatalytic activity. The photocatalytic activity of CeO_2-SiO_2 nanoparticles, which were prepared by 30 min irradiation times was found to have better performance than commercial reference P25.

1. Introduction

Dye pollutants from textile papers and other industries are important sources of environmental contamination. Conventional treatment of such wastewater generally involves coagulation/flocculation [1, 2], electrocoagulation [3], coagulation/carbon adsorption process [4], and so on. These methods, however, merely transfer dyes from the liquid phase to the solid phase, requiring further treatment and causing secondary pollution [5]. Photocatalytic degradation of them continues to attract interest as a method to mitigate their impact on the environment. When photocatalyst is excited, it produces photogenerated holes in the valence band and the photogenerated electrons in the conduction band. Photogenerated holes have strong oxidation power, which are widely studied for environmental cleaning [6–10]. One important application of photocatalyst in environment cleaning is degradation of organic pollutants in waste water, especially those from the textile and the photographic industries. The photocatalysis technology has several advantages over other processes, such as cost-effectiveness, the use of ultraviolet (UV), near-UV or solar light as energy source, no addition of other chemicals, the operation at near room temperature, the capability of efficiently mineralizing most organic compounds, and the simple implementation with other conventional technologies to form a hybrid system [11]. Among these catalysts, TiO_2 has been proved to be a competent photocatalyst for environmental applications because of its strong oxidizing ability, nontoxicity, and long-term stability [6–10]. However, TiO_2 with a band gap of 3.0–3.2 eV can be photoexcited under irradiation of UV light ($\lambda < 395$ nm), which is only about 2–4% of sunlight [12].

Table 1: The calculated average crystallite sizes of CeO_2-SiO_2 samples.

Sample	Average crystallite sizes (nm)
M-30 min	8
M-60 min	10
M-90 min	11
M-120 min	12
M-180 min	14
H-24 h	15
P_{25}	25

Therefore, considerable effort has been made to increase the absorption of TiO_2 in the visible region to improve its visible light response through various surface modifications such as doping of various metal or metal oxides [13–17].

Dyes such as methylene blue (MB) are the main organic pollutants from dyeing and printing, textile industries, paper and ink manufacturing industries, cosmetics, pharmaceuticals, denim industries, food industries, and so on [18]. Methylene blue (MB), a common organic dye, was selected as a target compound because MB is ubiquitously used and the removal of the dye from wastewaters has been an acute problem [19]. Li et al. found that, during liquid-phase photocatalytic degradation of MB under visible light irradiation (>420 nm), the as-prepared S-doped TiO_2 exhibited much higher activity than pure TiO_2 [20].

We know that a rare-earth oxide such as CeO_2 has been applied widely in many fields. The applications of ceria are in solid oxide fuel cells, oxygen gas sensors, fluorescent materials, acting as the three-way catalysts in vehicle emission control systems, ultraviolet blocking materials, gates for metal-oxide semiconductor devices and phosphors, and so forth [21–24]. Furthermore, nanocrystalline CeO_2-based materials not only benefit from those applications, but also possess some unique properties, including lattice expansion [25], transition from boundary diffusion to lattice diffusion [26], and blue shift in ultraviolet absorption spectra [27]. Therefore, it is of critical importance to regulate the size and shape to explore its novel applications and properties. Up to now, big efforts have been devoted to the chemical synthesis of CeO_2 nanomaterials with various morphologies and sizes, such as porous structures, films, nanoparticles, and so forth [28–44]. The development of efficient methods to synthesize nanostructures with well-defined size and shape is one of the key trends in material chemistry because of their size/shape-dependent properties and potential applications. In the past few years, some effective methods have been developed to prepare monodispersed CeO_2 with different shapes. For example, nanocubes were prepared by a two-step precipitation method using oleic acid as a capping agent [45], nanopolyhedrals and nanocubes were synthesized via the decanoic acid-assisted supercritical hydrothermal process at 400°C [46], and nanopolyhedrons were obtained by the thermolysis reaction of cerium benzoylacetonate complex in oleic acid/oleylamine solvents under vacuum condition at 310–330°C [47]. However, the above methods required complicated procedure, special equipments, or organometallic precursor. So it still remains a great challenge to fabricate ceria nanocrystals with uniform size and well-defined crystal shape by a simple and economical method. Here in this study, we report the synthesis of nanocrystalline CeO_2-SiO_2 by a microwave-assisted irradiation process for the first time. The synthesized nanocrystalline CeO_2-SiO_2 samples were characterized by X-ray diffraction (XRD) technique, Brunauer-Emmett-Teller (BET) surface measurements, transmission electron microscopy (TEM), and UV-vis diffuse reflectance spectra (UV-vis DRS). The photocatalytic activities of CeO_2-SiO_2 were investigated by the degradation of methylene blue dye under the irradiations of UV light.

2. Experimental

The dye under investigation, namely, methylene blue (MB), with a labeled purity of more than 90% was obtained from Sigma-Aldrich and used as received. Deionized water was used to make the dye solutions of desired concentration.

2.1. Catalyst Preparation and Characterization. All chemicals were of reagent grade without further purification. Ce-Si binary oxide was synthesized by a microwave method according to the following procedure: 1.4 g hexadecyltrimethylammonium bromide (CTAB) was added gradually to 10 g tetraethyl orthosilicate (TEOS, Aldrich) solution and the mixture was stirred at 60°C for 10 min till the CTAB was completely dissolved. 2.5 g of hexahydrated cerium nitrate ($Ce(NO_3)_3$-$6H_2O$, Alfa Aesar) dissolved in ethanol (18.0 g) was subsequently added to the mixture of CTAB and TEOS and continually stirred for further 10 min at 60°C. The solution was cooled to room temperature and 1 mL aqueous HCl (0.05 mol L^{-1}) was added and stirred for 2 h. The above mixtures were poured into the Teflon lined digestion vessel, where vessel cover acts as an overpressure release valve surrounded by a safety shield and then heated by a microwave synthesizer (ETHOS TC from Milestone Inc.) and maintained at 160°C for different times.

The resultant precipitates were collected by centrifugation, washed by the deionized water and then dried at 80°C for 24 h to gain precursors.

At last, the precursors were heat treated at 500°C for about 4 h at a ramping rate of 0.5°C min^{-1} to obtain CeO_2-SiO_2. The samples obtained under 30, 60, 90, 120, and 180 min microwave irradiation are denoted as M-30 min, M-60 min, M-90 min, M-120 min, and M-180 min, respectively. As a comparative study, a conventional hydrothermal process was used as a preparation method (H, reaction temperature: 160°C, reaction time: 24 h, calcination temperature: 500°C for 4 h at a ramping rate of 0.5°C min^{-1}). The obtained CeO_2-SiO_2 sample was denoted as H-24 h. TiO_2 P_{25} from Degussa was employed as a standard photocatalyst for comparison purpose. It consists of mainly anatase phase (ca. 80%), non-porous polyhedral particles of ca. 25 nm mean size, and a BET surface area of ca. 50 m^2 g^{-1}.

2.2. Characterization. To determine the crystallite sizes and identities of CeO_2-SiO_2, all the samples were characterized by

Table 2: Texture parameters of CeO_2-SiO_2 samples.

Sample	S_{BET} (m^2/g)	S_t (m^2/g)	S_{micro} (cm^2/g)	S_{ext} (cm^2/g)	V_p (cm^3/g)	V_{micro} (cm^3/g)	V_{meso} (cm^3/g)	r (Å)
M-30 min	335	340	240	95	0.59	0.090	0.500	5.58
M-60 min	300	320	210	90	0.58	0.085	0.495	5.57
M-90 min	236	250	170	66	0.44	0.050	0.390	5.56
M-120 min	118	130	95	23	0.30	0.040	0.260	5.55
M-180 min	100	110	85	15	0.28	0.030	0.250	5.54
H-24 h	90	10	77	13	0.26	0.020	0.240	5.53
P_{25}	50	—	—	—	—	—	—	—

Table 3: The band gap energy of CeO_2-SiO_2 samples.

Sample	Band gap energy (eV)
M-30 min	3.25
M-60 min	3.32
M-90 min	3.42
M-120 min	3.55
M-180 min	4.02
H-24 h	4.10

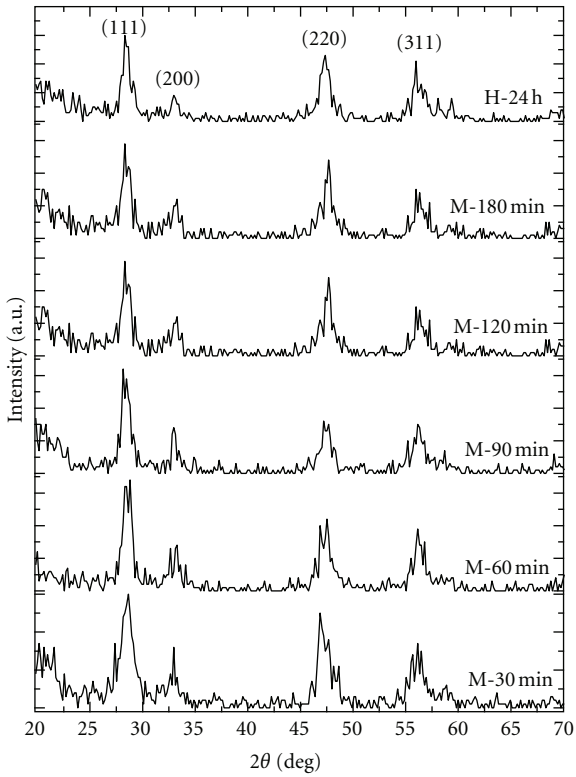

Figure 1: X-ray diffraction patterns of CeO_2-SiO_2 samples prepared by different irradiation times and hydrothermal method.

X-ray diffraction (XRD), transmission electron microscope (TEM), and UV-vis diffuse reflectance spectra (UV-vis DRS). The XRD measurements were performed on a Rigaku X-ray diffractometer system equipped with as RINT 2000 wide-angle goniometer using Cu Kα radiation and a power of 40 kV × 30 mA. The intensity data were collected at 25°C over a 2θ range of 10–80°. TEM images were obtained on Hitachi H-9500 operated at 300kv. UV-vis diffuse reflectance absorption spectra were recorded in air at room temperature in the wavelength range of 200–800 nm using a Shimadzu UV-2450 at 295 K. The Brunauer-Emmet-Teller (BET) surface areas were determined from N_2-adsorption measurements at 77 K using Nova 2000 series, Chromatech. Prior to analysis, the samples were outgased at 250°C for 4 h.

2.3. Photocatalytic Activity Measurements. A set of photocatalytic degradation experiments of methylene blue (100 ppm) was carried out by photoreactor under UV light irradiation. The light source for photocatalysis was a mercury lamp (150 W high pressure). The catalysts and solution were separated by filtration; the collected samples were analyzed by UV-Vis spectrophotometer (Shimadzu UV-2450). The photodegradation efficiency of methylene blue has been calculated by applying the following equation:

$$\%\text{photodegradation efficiency} = \frac{(C_o - C)}{C_o} \times 100, \quad (1)$$

where C_o is the original methylene blue content, C is the retained methylene blue in solution.

3. Results and Discussion

3.1. Evaluation and Characterization of Synthesized Materials

3.1.1. Phase Analysis. All the obtained peaks in the pattern of Figure 1 belong only to CeO_2. No other peaks related to impurities were detected, which confirm that the synthesized nanoparticles are pure CeO_2 with cubic phase [47]. It was observed from the XRD patterns that with the increase of the treatment time, intensity of XRD peaks increased and full width at half maximum decreased, indicating the enhancement of the crystallinity and crystallite size. Compared with the conventional hydrothermal route, the irradiation under the microwave produces a better crystallinity in a shorter treatment time (30 min), which is a good evidence that the introduction of the microwave really can save energy and time with faster kinetics of crystallization [48–50]. The particle sizes were calculated from (1 1 1) peak using Scherrer's formula $D = k\lambda/\beta\cos\theta$, where D is the average grain size, k a constant equal to 0.89, λ the wavelength of X-rays and β is the corrected half width. The calculated average crystallite sizes of the samples are tabulated in Table 1.

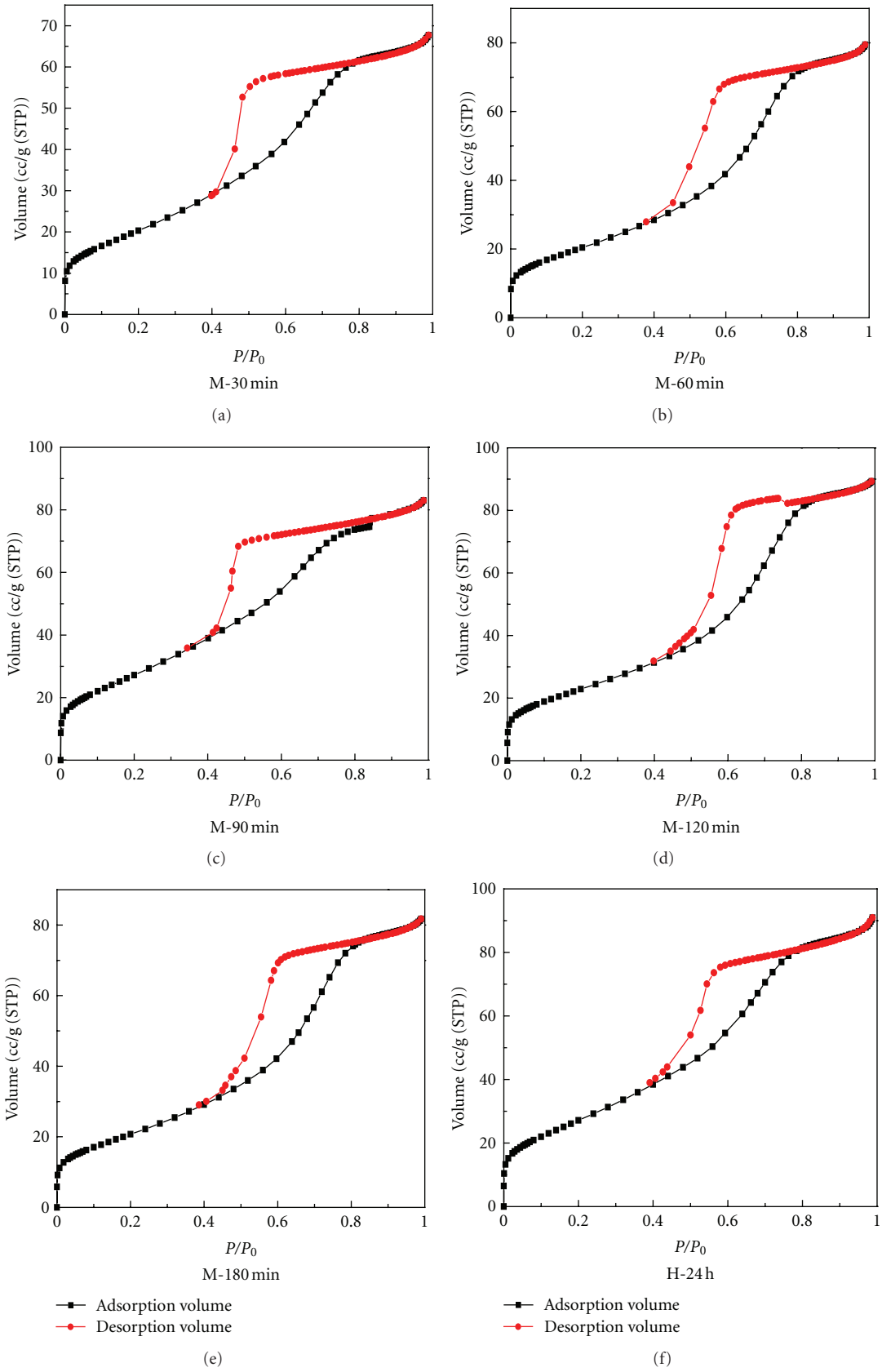

FIGURE 2: N_2 adsorption and desorption isotherm for CeO_2-SiO_2 samples prepared by different irradiation times and hydrothermal method.

Table 4: Effect of CeO_2-SiO_2 nanoparticles on the photoactivity.

Sample	S_{BET} (m^2/g)	Band gap eV	MB removal efficiency, %	V_p (cm^3/g)	Crystallite size, nm
M-30 min	335	3.25	93	0.59	8
M-60 min	300	3.32	90	0.58	10
M-90 min	236	3.42	89	0.44	11
M-120 min	118	3.55	88	0.30	12
M-180 min	100	4.02	87	0.28	14
H-24 h	90	4.10	85	0.26	15

Table 5: Effect of pH of MB solution on MB removal efficiency.

pH of MB	MB removal efficiency, %
3	93.0
4	95.0
7	96.0
9	96.2

Table 6: Effect of MB concentration on MB removal efficiency.

MB concentration, ppm	MB removal efficiency, %
100	96.0
150	96.0
200	96.0
300	90.0
400	95.0

3.1.2. Surface Area Analysis. The CeO_2-SiO_2 samples are characterized by specific surface area S_{BET} as shown in Table 2, which indicates that the increase of irradiation time decreases surface area and surface area of sample prepared by microwave method is higher than that prepared by the hydrothermal method. The parameters of surface area and the data calculated from the *t*-plot are collected in Table 2. The obtained results from the N_2-adsorption isotherms for CeO_2-SiO_2 samples indicate that both are typical of mesoporous solids type IV as shown in Figure 2. However, a decrease in the adsorption capacity of the CeO_2-SiO_2 samples was observed after increase irradiation time of the microwave. Furthermore, it was noticed that the total pore volume of M-30 min sample had the highest value. The values of S_{BET} and S_t are generally close in most samples indicating the presence of mesopores.

3.1.3. UV-Vis-DRS Analysis. The optical properties of synthesized CeO_2-SiO_2 samples were examined by UV-visible spectrophotometer, and the results are displayed in Figure 3. The results reveal an increase in absorbency in the visible light region parallel to the declining irradiation time of the examined systems. Therefore, the study of UV-vis radiation absorption is an important tool for the evaluation of the changes in the produced semiconductor materials by different treatments. Further, the band gap energy was calculated on the basis of the maximum absorption band of CeO_2-SiO_2 nanoparticles according to (2).

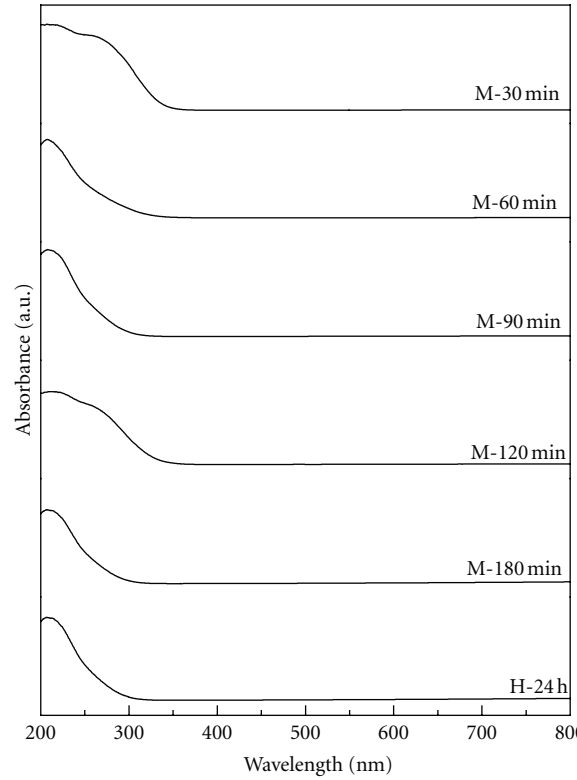

Figure 3: UV-vis spectra of CeO_2-SiO_2 samples prepared by different irradiation times and hydrothermal method.

$$Eg = \frac{1240}{\lambda}, \tag{2}$$

where *Eg* is the band gap energy, and λ is the lower cutoff wavelength (nm) of the photocatalyst. The values of *Eg*, the band gap of the CeO_2-SiO_2 samples, are compiled in Table 3.

3.1.4. TEM Observation. With the aid of transmission electron microscope, size and morphology of as-synthesized samples were recorded. Based on the results of photocatalytic activity as given in Section 3.2.1, the highest catalytic activity was observed for the sample M-30, and the respective samples M-30 and H-24 were subjected to TEM analysis. The corresponding TEM analysis is shown in Figures 4(a) and 4(b). The results show that the shape of

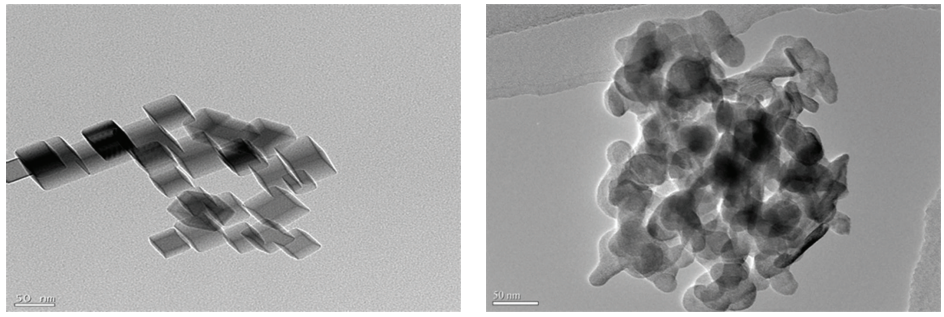

(a) (b)

Figure 4: TEM images of CeO_2-SiO_2 samples prepared by (a) 30 min different irradiation times and (b) hydrothermal method.

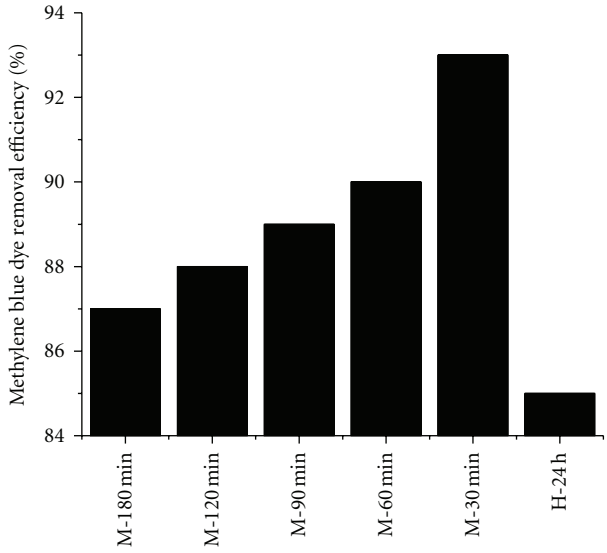

Figure 5: Effect of irradiation time and preparation method on photocalytic efficiency percentage of methylene blue dye.

the CeO_2-SiO_2 sample prepared by hydrothermal method is spherical shape particles with size of about 15 nm. But the shape of CeO_2-SiO_2 sample prepared by microwave method for 30 min irradiation time is nanocubes with size of about 8 nm. These findings suggest that the shape and size of nanoparticles depend essentially on the preparation method.

3.2. Evaluation of Photocatalytic Activity

3.2.1. Effect of Preparation Method and Irradiation Time on Photocatalytic Degradation of Methylene Blue Dye. Within the frame of the present study, the photocatalytic degradation of methylene blue dye was taken as a probe reaction to test the catalytic activity of the system under consideration and Figure 5 shows the effect of irradiation time and preparation method on photocatalytic oxidation of methylene blue dye.

A keen insight into the obtained results, one could observe the following.

The highest value of degradation was M-30. The variation in activity should be due to the differences in physical properties such as band gap, particle size, and surface texture. The photocatalytic activities in relation to other obtained physical properties (S_{BET}, band gap, V_p, and crystallite sizes) are compiled in Table 4.

A maximum photocatalytic activity is found for M-30, where the surface area and pore volume own the maximum values counter to the band gap values. One could explain such increase due to a decrease in energy to exit electron from conduction band to valence band. Also, the M-30 min has the best photoactivity, since it has the lowest band gap and particle size and the highest surface area and pore volume.

3.2.2. Factors Affecting on Photocatalytic Activity

Effect of pH. A series of experiments has been carried out to study the effect of pH on MB removal efficiency under the following conditions: 0.3 g/L catalyst/MB solution ratio, 100 ppm Conc. of MB, and 1 h reaction time. The findings are summarized in Table 5. The results indicate that increasing the pH of MB solution from 3 to 7 leads to an increase in MB removal efficiency from 93 to 96.0%, but at pH more than 7, the MB removal efficiency almost remains unchanged. The possible reason for this behavior is that alkaline pH range favours the formation of more OH radical due to the presence of large quantity of OH^- ions in the alkaline medium, which enhances the photocatalytic degradation of MB significantly [51]. The optimum condition for pH is 7 at which photodegradation percentage of MB reach to 96%.

Effect of MB Concentration. A series of experiments has been carried out to study the effect of the MB concentration on MB removal efficiency under the aforementioned conditions at pH 7. The results are summarized in Table 5. It can be seen that increasing MB concentration from 100 to 200 ppm has no significant effect on MB removal efficiency, but at a concentration higher than 200 ppm, the MB removal efficiency was decreased. The optimum condition for MB concentration is 200 ppm at MB removal efficiency of 96% (see Table 6).

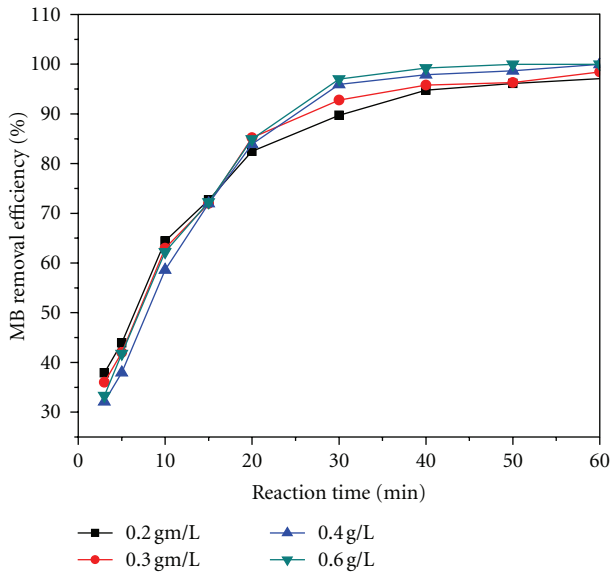

Figure 6: Effect of loading of optimum CeO_2-SiO_2 sample on MB removal efficiency percentage.

Effect of Catalyst/MB Solution Ratio. A series of experiments has been carried out to study the effect of catalyst/MB solution ratio g/L on MB removal efficiency under the aforementioned conditions at MB concentration of 200 ppm. The findings are shown in Figure 6. The results indicate that increasing the catalyst/MB solution ratio from 0.2 to 0.4 g/L leads to an increase in MB removal efficiency from 96.0 to 99.9%, respectively, but at a catalyst/MB solution ratio more than 0.4 g/L the MB removal efficiency almost remains unchanged. The optimum condition of catalyst/MB solution ratio g/L is 0.4 at 99.9% MB removal efficiency.

Comparison between Photocatalytic Activity of CeO_2-SiO_2 and TiO_2 Degussa. Finally, in the present study, a series of experiments has been carried out in order to compare the photocatalytic activity of optimum sample (M-30 min) and commercial reference P25 under the following conditions: 0.4 g/L catalyst/MB solution ratio, 200 ppm Conc. of MB, and 1 h reaction time. We found the photocatalytic activity of M-30 min and P25 are 99.9 and 94%, respectively. Therefore, the photocatalytic activity of CeO_2-SiO_2 nanoparticles which prepared by 30 min irradiation time was found to have a better performance than the commercial reference P25. Because the surface area of CeO_2-SiO_2 (335 m^2/gm) is higher than that of P25 (50 m^2/gm). It is concluded that the synthesized CeO_2-SiO_2 is one of the best candidate for environmental applications as a photocatalyst.

4. Conclusion

The microwave method is a useful for the preparation of CeO_2-SiO_2 nanoparticles with high photocatalytic activity, high surface area, and desirable pore structures. The irradiation time showed significant effect on the texture structure, band gap, and particle size. These physical changes affected the efficiency of the photo degradation of methylene blue dye. The activity is well correlated with the band gap, surface area and pore volume. The CeO_2-SiO_2 nanoparticles, which were prepared for 30 min irradiation times exhibited the highest photoactivity due to its high surface area, large pore volume, small particle size, and small band gap. The photocatalytic activity of CeO_2-SiO_2 nanoparticles, which were prepared for 30 min irradiation time was found to have a better performance than commercial reference P25. It is concluded that the synthesized CeO_2-SiO_2 is one of the best candidate for environmental applications as a photocatalyst.

References

[1] C. Allegre, M. Maisseu, F. Charbit, and P. Moulin, "Coagulation-flocculation-decantation of dye house effluents: concentrated effluents," *Journal of Hazardous Materials*, vol. 116, no. 1-2, pp. 57–64, 2004.

[2] V. Golob, A. Vinder, and M. Simonič, "Efficiency of the coagulation/flocculation method for the treatment of dyebath effluents," *Dyes and Pigments*, vol. 67, no. 2, pp. 93–97, 2005.

[3] A. Alinsafi, M. Khemis, M. N. Pons et al., "Electro-coagulation of reactive textile dyes and textile wastewater," *Chemical Engineering and Processing: Process Intensification*, vol. 44, no. 4, pp. 461–470, 2005.

[4] S. Papic, N. Koprivanac, A. LoncaricBozic, and A. Metes, "Removal of some reactive dyes from synthetic wastewater by combined Al(III) coagulation/carbon adsorption process," *Dyes and Pigments*, vol. 62, no. 3, pp. 291–298, 2004.

[5] K. Tanaka, K. Padermpole, and T. Hisanaga, "Photocatalytic degradation of commercial azo dyes," *Water Research*, vol. 34, no. 1, pp. 327–333, 2000.

[6] M. R. Hoffmann, S. T. Martin, W. Choi, and D. W. Bahnemann, "Environmental applications of semiconductor photocatalysis," *Chemical Reviews*, vol. 95, no. 1, pp. 69–96, 1995.

[7] C. H. Li, Y. H. Hsieh, W. T. Chiu, C. C. Liu, and C. L. Kao, "Study on preparation and photocatalytic performance of Ag/TiO_2 and Pt/TiO_2 photocatalysts," *Separation and Purification Technology*, vol. 58, no. 1, pp. 148–151, 2007.

[8] D. F. Ollis and C. S. Turchi, "Heterogeneous photocatalysis for water purification: contaminant mineralization kinetics and elementary reactor analysis," *Environmental Progress*, vol. 9, no. 4, pp. 229–234, 1990.

[9] F. B. Li, X. Z. Li, and M. F. Hou, "Photocatalytic degradation of 2-mercaptobenzothiazole in aqueous La^{3+}-TiO_2 suspension for odor control," *Applied Catalysis B*, vol. 48, no. 3, pp. 185–194, 2004.

[10] F. B. Li and X. Z. Li, "Photocatalytic properties of gold/gold ion-modified titanium dioxide for wastewater treatment," *Applied Catalysis A*, vol. 228, no. 1-2, pp. 15–27, 2002.

[11] T. D. Nguyen-Phan and E. W. Shin, "Morphological effect of TiO_2 catalysts on photocatalytic degradation of methylene blue," *Journal of Industrial and Engineering Chemistry*, vol. 17, no. 3, pp. 397–400, 2011.

[12] C. B. Almquist and P. Biswas, "Role of synthesis method and particle size of nanostructured TiO_2 on its photoactivity," *Journal of Catalysis*, vol. 212, no. 2, pp. 145–156, 2002.

[13] K. Aoki, Y. Takeuchi, and Y. Amao, "Visible-light sensitisation of nanocrystalline TiO_2 film by Mg chlorophyll-a through the axial imidazole-4-acetic acid ligand," *Bulletin of the Chemical Society of Japan*, vol. 78, no. 1, pp. 132–134, 2005.

[14] S. Sakthivel, M. V. Shankar, M. Palanichamy, B. Arabindoo, D. W. Bahnemann, and V. Murugesan, "Enhancement of photocatalytic activity by metal deposition: characterisation and photonic efficiency of Pt, Au and Pd deposited on TiO_2 catalyst," *Water Research*, vol. 38, no. 13, pp. 3001–3008, 2004.

[15] C. G. Wu, C. C. Chao, and F. T. Kuo, "Enhancement of the photo catalytic performance of TiO_2 catalysts via transition metal modification," *Catalysis Today*, vol. 97, no. 2-3, pp. 103–112, 2004.

[16] Y. Q. Wu, G. X. Lu, and G. X. Li, "The long-term photocatalytic stability of Co^{2+}-modified P25-TiO_2 powders for the H_2 production from aqueous ethanol solution," *Journal of Photochemistry and Photobiology A*, vol. 181, no. 2-3, pp. 263–267, 2006.

[17] R. M. Mohamed and I. A. Mkhalid, "The effect of rare earth dopants on the structure, surface texture and photocatalytic properties of TiO_2-SiO_2 prepared by sol-gel method," *Journal of Alloys and Compounds*, vol. 501, no. 1, pp. 143–147, 2010.

[18] M. A. Brown and S. C. de Vito, "Predicting azo dye toxicity," *Critical Reviews in Environmental Science and Technology*, vol. 23, no. 3, pp. 249–324, 1993.

[19] H. Gnaser, M. R. Savina, W. F. Calaway, C. E. Tripa, I. V. Veryovkin, and M. J. Pellin, "Photocatalytic degradation of methylene blue on nanocrystalline TiO_2: surface mass spectrometry of reaction intermediates," *International Journal of Mass Spectrometry*, vol. 245, no. 1–3, pp. 61–67, 2005.

[20] H. X. Li, X. Y. Zhang, Y. N. Huo, and J. Zhu, "Supercritical preparation of a highly active S-doped TiO_2 photocatalyst for methylene blue mineralization," *Environmental Science & Technology*, vol. 41, no. 12, pp. 4410–4414, 2007.

[21] Q. Fu, H. Saltsburg, and M. Flytzani-Stephanopoulos, "Active nonmetallic Au and Pt species on ceria-based water-gas shift catalysts," *Science*, vol. 301, no. 5635, pp. 935–938, 2003.

[22] E. P. Murray, T. Tsai, and S. A. Barnett, "A direct-methane fuel cell with a ceria-based anode," *Nature*, vol. 400, no. 6745, pp. 649–651, 1999.

[23] A. Corma, P. Atienzar, H. García, and J. Y. Chane-Ching, "Hierarchically mesostructured doped CeO_2 with potential for solar-cell use," *Nature Materials*, vol. 3, no. 6, pp. 394–397, 2004.

[24] A. H. Morshed, M. E. Moussa, S. M. Bedair, R. Leonard, S. X. Liu, and N. El-Masry, "Violet/blue emission from epitaxial cerium oxide films on silicon substrates," *Applied Physics Letters*, vol. 70, no. 13, pp. 1647–1649, 1997.

[25] B. S. Liu, X. J. Zhao, N. Z. Zhang, Q. N. Zhao, X. He, and J. Y. Feng, "Photocatalytic mechanism of TiO_2-CeO_2 films prepared by magnetron sputtering under UV and visible light," *Surface Science*, vol. 595, no. 1–3, pp. 203–211, 2005.

[26] X. D. Zhou, W. Huebner, and H. U. Anderson, "Processing of nanometer-scale CeO_2 particles," *Chemistry of Materials*, vol. 15, no. 2, pp. 378–382, 2003.

[27] X. D. Zhou, W. Huebner, and H. U. Anderson, "Room-temperature homogeneous nucleation synthesis and thermal stability of nanometer single crystal CeO_2," *Applied Physics Letters*, vol. 80, no. 20, pp. 3814–3816, 2002.

[28] S. Tsunekawa, T. Fukuda, and A. Kasuya, "Blue shift in ultraviolet absorption spectra of monodisperse CeO_{2-x} nanoparticles," *Journal of Applied Physics*, vol. 87, no. 3, pp. 1318–1321, 2000.

[29] A. Corma, P. Atienzar, H. García, and J. Y. Chane-Ching, "Hierarchically mesostructured doped CeO_2 with potential for solar-cell use," *Nature Materials*, vol. 3, no. 6, pp. 394–397, 2004.

[30] D. Terribile, A. Trovarelli, J. Llorca, C. de Leitenburg, and G. Dolcetti, "The synthesis and characterization of mesoporous high-surface area ceria prepared using a hybrid organic/inorganic route," *Journal of Catalysis*, vol. 178, no. 1, pp. 299–308, 1998.

[31] D. M. Lyons, K. M. Ryan, and M. A. Morris, "Preparation of ordered mesoporous ceria with enhanced thermal stability," *Journal of Materials Chemistry*, vol. 12, no. 4, pp. 1207–1212, 2002.

[32] C. Ho, J. C. Yu, T. Kwong, A. C. Mak, and S. Lai, "Morphology-controllable synthesis of mesoporous CeO_2 nano- and microstructures," *Chemistry of Materials*, vol. 17, no. 17, pp. 4514–4522, 2005.

[33] H. I. Chen and H. Y. Chang, "Synthesis of nanocrystalline cerium oxide particles by the precipitation method," *Ceramics International*, vol. 31, no. 6, pp. 795–802, 2005.

[34] A. Bumajdad, M. I. Zaki, J. Eastoe, and L. Pasupulety, "Microemulsion-based synthesis of CeO_2 powders with high surface area and high-temperature stabilities," *Langmuir*, vol. 20, no. 25, pp. 11223–11233, 2004.

[35] D. S. Bae, B. Lim, B. I. Kim, and K. S. Han, "Synthesis and characterization of ultrafine CeO_2 particles by glycothermal process," *Materials Letters*, vol. 56, no. 4, pp. 610–613, 2002.

[36] M. Lundberg, B. Skårman, F. Cesar, and L. R. Wallenberg, "Mesoporous thin films of high-surface-area crystalline cerium dioxide," *Microporous and Mesoporous Materials*, vol. 54, no. 1-2, pp. 97–103, 2002.

[37] J. P. Nair, E. Wachtel, I. Lubomirsky, J. Fleig, and J. Maier, "Anomalous expansion of CeO_2 nanocrystalline membranes," *Advanced Materials*, vol. 15, no. 24, pp. 2077–2081, 2003.

[38] B. Tang, L. H. Zhuo, J. C. Ge, G. L. Wang, Z. Q. Shi, and J. Y. Niu, "A surfactant-free route to single-crystalline CeO_2 nanowires," *Chemical Communications*, no. 28, pp. 3565–3567, 2005.

[39] D. S. Zhang, H. X. Fu, L. Y. Shi et al., "Synthesis of CeO_2 nanorods via ultrasonication assisted by polyethylene glycol," *Inorganic Chemistry*, vol. 46, no. 7, pp. 2446–2451, 2007.

[40] G. Z. Chen, C. X. Xu, X. Y. Song, W. Zhao, Y. Ding, and S. X. Sun, "Interface reaction route to two different kinds of CeO_2 nanotubes," *Inorganic Chemistry*, vol. 47, no. 2, pp. 723–728, 2008.

[41] D. Zhang, H. Fu, L. Shi, J. Fang, and Q. Li, "Carbon nanotube assisted synthesis of CeO_2 nanotubes," *Journal of Solid State Chemistry*, vol. 180, no. 2, pp. 654–660, 2007.

[42] K. L. Yu, G. L. Ruan, Y. H. Ben, and J. J. Zou, "Convenient synthesis of CeO_2 nanotubes," *Materials Science and Engineering B*, vol. 139, no. 2-3, pp. 197–200, 2007.

[43] K. B. Zhou, Z. Q. Yang, and S. Yang, "Highly reducible CeO_2 nanotubes," *Chemistry of Materials*, vol. 19, no. 6, pp. 1215–1217, 2007.

[44] K. Kaneko, K. Inoke, B. Freitag et al., "Structural and morphological characterization of cerium oxide nanocrystals prepared by hydrothermal synthesis," *Nano Letters*, vol. 7, no. 2, pp. 421–425, 2007.

[45] L. Qian, J. Zhu, W. Du, and X. Qian, "Solvothermal synthesis, electrochemical and photocatalytic properties of monodispersed CeO_2 nanocubes," *Materials Chemistry and Physics*, vol. 115, no. 2-3, pp. 835–840, 2009.

[46] S. W. Yang and L. Gao, "Controlled synthesis and self-assembly of CeO_2 nanocubes," *Journal of the American Chemical Society*, vol. 128, no. 29, pp. 9330–9331, 2006.

[47] J. Zhang, S. Ohara, M. Umetsu, T. Naka, Y. Hatakeyama, and T. Adschiri, "Colloidal ceria nanocrystals: a tailor-made crystal

morphology in supercritical water," *Advanced Materials*, vol. 19, no. 2, pp. 203–206, 2007.

[48] R. Si, Y. W. Zhang, L. P. You, and C. H. Yan, "Rare-earth oxide nanopolyhedra, nanoplates, and nanodisks," *Angewandte Chemie International Edition*, vol. 44, no. 21, pp. 3256–3260, 2005.

[49] F. Niu, D. Zhang, L. Shi, X. He, H. Li, and H. Mai, "Facile synthesis, characterization and low-temperature catalytic performance of Au/CeO_2 nanorods ," *Materials Letters*, vol. 63, no. 24-25, pp. 2132–2135, 2009.

[50] S. Komarneni, R. Roy, and Q. H. Li, "Microwave-hydrothermal synthesis of ceramic powders," *Materials Research Bulletin*, vol. 27, no. 12, pp. 1393–1405, 1992.

[51] S. F. Liu, I. R. Abothu, and S. Komarneni, "Barium titanate ceramics prepared from conventional and microwave hydrothermal powders," *Materials Letters*, vol. 38, no. 5, pp. 344–350, 1999.